Nuclear Medicine Communications

Original article

The diagnostic performance of 99mTc-methionine single-photon emission tomography in grading glioma preoperatively: a comparison with histopathology and Ki-67 indices

Nisha Rani[a], Baljinder Singh[a], Narendra Kumar[b], Paramjit Singh[c], Puja P. Hazari[d], Ambika Jaswal[d], Sunil K. Gupta[e], Rajesh Chhabra[e], Bishan D. Radotra[f] and Anil K. Mishra[d]

Objective **To characterize glioma preoperatively using quantitative 99mTc-methionine SPECT and comparison with MR-perfusion/spectroscopy and histopatholgical/ Ki-67 scoring.**

Methods **Twenty-nine patients (21M: 8F; mean age 42.3 ± 10.5 years) with clinical and radiological suspicion of glioma assessed by 99mTc-MDM/SPECT and ceMRI. Additionally, 12/29 patients underwent dynamic susceptibility contrast-enhanced (DSCE) MRI and magnetic resonance spectroscopy (MRS) examination. Three patients with benign pathologies were recruited as controls. Histopathological tumor analysis was done in all ($n = 29$) the patients, and the Ki-67 index was evaluated in 20/29 patients. The target-to-nontarget (T/NT) methionine tumor uptake ratios, normalized cerebral blood volume (nCBV) and metabolites [choline/N-acetyl aspartate (Cho/ NAA), Cho/creatine (Cr), Cr/NAA and Cr/Cho) ratios were measured in tumor areas.**

Results **On histopathological analysis, 26/29 patients had glioma (G IV-13; G III-04; G II-09). The mean T/NT ratio in G-II was significantly lower (2.46 ± 2.3) than in G-III (7.13 ± 2.2) and G-IV (5.16 ± 1.2). However, the mean ratio was highest (15.9 ± 6.8) in meningioma (n=3). The T/NT cutoff ratio of 3.08 provided 100% sensitivity, 87.5% specificity for discriminating high-grade glioma (HGG) from low-grade glioma (LGG) disease. Likewise, the nCBV cutoff of 2.43 offered 100% sensitivity and 80% specificity. Only the Cho/NAA cutoff value of greater than 3.34 provided reasonable sensitivity and specificity of 85.7% and 80.0% respectively for this differentiation. T/NT ratio correlated significantly with nCBV and Cho/NAA, Cho/Cr ratios but not with Ki-67.**

Conclusion **Quantitative 99mTc-MDM -SPECT provided high sensitivity and specificity to differentiate HGG versus LGG preoperatively and demonstrated a potential role for the differential diagnosis of glial versus nonglial tumors.**

Nuclear Medicine Communications 2020, **41**:848–857

Keywords: 99mTc-methionine single-photon emission tomography, dynamic susceptibility contrast-enhanced-MRI, glioma, grading, Ki-67, magnetic resonance spectroscopy

Departments of [a]Nuclear Medicine, [b]Radiotherapy, [c]Radio-diagnosis and Imaging, PGIMER, Chandigarh, [d]Division of Cyclotron and Radiopharmaceutical Sciences, Institute of Nuclear Medicine and Allied Science, DRDO, New Delhi, Departments of [e]Neurosurgery and [f]Histopathology, PGIMER, Chandigarh, India

Correspondence to Dr. Baljinder Singh, PhD, Department of Nuclear Medicine, PGIMER, Chandigarh 160012, India
Tel: +91 172 2756725/+91 99142 09725; fax: +91 172 2744401;
e-mail: drbsingh5144@gmail.com

Received 12 February 2020 **Accepted** 6 May 2020

Introduction

Primary brain tumors remain a significant health problem worldwide, with an estimated incidence of approximately 14 cases per 100 000 people in the United States [1]. The projected survival for a glioma patient is based upon the tumor grading and associated indices like Ki-67 proliferation index determined by histopathology examination which is often sampled by stereotactic biopsy. However, as the gliomas are often heterogeneous; therefore, the biopsied sample may not reflect the true malignant potential of glioma [2]. Various imaging markers have been reported as prognostic indicators for determining the pathological grading of glioma. There is growing evidence for the use of advanced multimodality MRI and PET to provide a noninvasive critical insight into the underlying molecular characteristics of gliomas [3,4]. Dynamic susceptibility contrast-enhanced (DSCE) MR imaging assesses tumor vascularity and magnetic resonance spectroscopy (MRS), which investigates metabolites' changes in tumor tissue, are the most widely used MRI techniques in glioma grading and prognostication [5,6].

Among the PET tracers, methionine labeled with Carbon-11 has been extensively used as the 'standard of care' for glioma imaging [7]. 11C-methionine transport through the energy-dependent L-type amino acid transporter (LAT-1) receptors [8]. LAT1 need an additional

DOI: 10.1097/MNM.0000000000001230

membrane-spanning protein antigen (4F2hc/CD98) for their functional expression and 4F2 antigen (CD98) has been reported to associate with various cellular activities including cellular proliferation [9,10]. Also, a significant correlation was observed between methionine uptake and Ki-67 proliferation index [11]. However, because of the prerequisite of an onsite cyclotron due to the short physical half-life of 20 min and cumbersome radiolabeling procedure, 11C-methonine could not become a routine PET imaging tracer, especially in highly busy centers [8]. To overcome such logistic concerns, we in the present study used 99mTc-methionine (99mTc-MDM) single-photon emission tomography (SPECT) tracer (an amino acid analog) which has a similar mechanism of uptake as that of 11C-MET [12,13]. 99mTc-MDM imaging has an advantage of allowing delayed imaging due to its longer half-life of 6 h which makes possible the detailed tumor characterization by serial (early and late phase) imaging [12]. The preclinical and clinical studies in treated gliomas have demonstrated that this newly developed radioligand has immense translational and clinical relevance [13,14]. With this background, the present study was carried out to evaluate the diagnostic performance of quantitative 99mTc-MDM SPECT in grading glioma preoperatively. The SPECT findings were compared with quantitative MR perfusion/spectroscopy parameters, histopathology and Ki-67 indices.

Methods

Patients:

In this study, 29 (21M:8F; mean age 42.5 ± 10.3 years; range 24–65 years) adult patients with clinical/radiological suspicion for glioma were recruited prospectively between September 2017 and July 2019. All the patients underwent 99mTc-MDM SPECT and conventional MR imaging followed by surgery. A subset of 12 (12/29) patients underwent DSCE-MRI and MRS. Histopathological analysis was carried out in all the biopsied samples obtained during the surgical/biopsy procedure and additionally, immunohistochemistry (IHC, Ki-67 index) was evaluated in 20 (20/29) patients. The mean time difference between surgical biopsy procedure and 99mTc-MDM SPECT imaging studies was 4.58 ± 3.34 days. Additionally, three patients (two cerebral tuberculoma and one neurocysticercosis) were recruited as control cases to evaluate the uptake pattern of the radiotracer in non-neoplastic pathologies. The image findings were compared with the reference standard (histopathological findings). A written and informed consent was obtained from each patient and the study protocol was approved by the Institute Ethics Committee. Newly diagnosed adult patients (>18 years of age) of either sex (male or female) with clinical/radiological suspicion of glioma/primary brain tumors and having indications for surgery were included in the study. Patients with MRI contradictions, unstable or noncooperative patients were not included in the study.

99mTc-methionine single-photon emission tomography protocol and data processing

Reconstitution of a lyophilized single vial methionine kits was performed as described previously [13]. The radiolabeled preparation filtered through a 0.22-μm filter (Millipore, Bedford, Massachusetts, USA) to ensure sterility before injecting it into the patients. The radiolabeling efficiency of 99mTc-MDM was evaluated (by ITLC method) for each kit used in this study.

About, 555.0–740.0 MBq radioactivity of 99mTc-MDM was administrated intravenously and tomographic images were acquired 2 h postinjection using a dual-head (SPECT) gamma camera (Symbia-T16, Siemens, Erlangen, Germany) over 360° degree rotation (circular orbit) in 128 projections (20 s/projection) in 128 × 128 matrix with a zoom factor of 1.5. The patient's head was immobilized with the help of a restraining strap. During image acquisition, the energy of the SPECT gamma camera was centered at 140 KeV with an energy window of ±20.0%. Low-dose computed tomography (CT) acquisition was done for attenuation correction with CT parameters set at 60 mAs and 140.0 kVP, respectively.

SPECT images were reconstructed using an iterative reconstruction algorithm with a Butterworth smoothing filter. Subsequently, the reconstructed data were displayed in three planes (axial, sagittal and coronal) for visual localization of the lesions demonstrating focal and abnormal uptake of the radiotracer. The reconstructed SPECT (axial images) data were also subjected to a semiquantitative analysis.

A region of interest (ROI) was drawn manually around the lesion (with abnormal focus of radiotracer) and the identical ROI was drawn on the contralateral side of the normal area of the brain in the same section. The maximum counts per pixel were calculated in the lesion as well as in the background area. The counts per pixel were used to calculate the target-to-nontarget (T/NT) ratio of the radiotracer.

MRI protocols and data processing

MRI was performed by using 3.0-Tesla (Siemens, Verio, Erlangen, Germany) or 3.0-Tesla (Discovery TM MR750w GEM; GE Healthcare, Germany) whole body MR units equipped with the standard head coil. The protocol for glioma imaging for 3.0-Tesla (Siemens, Verio) consisted of following sequences: Axial T1 weighted imaging (TR/TE: 1800/3.8), Axial T2 weighted imaging (TR/TE: 6000/96, Coronal T2 weighted imaging (TR/TE: 9000/94), and FLAIR (TR/TE: 9000/94), whereas the protocol for the 3.0-Tesla (Discovery TM

MR750w GEM) consisted of: Axial FLAIR T2 imaging (TR/TE: 11000/100), Axial T2 PROPELLER (periodically rotated overlapping parallel lines with enhanced reconstruction) imaging (TR/TE: 4800/114), and SAG FSPGR BRAVO (Fast spoiled grass sequence) (TR/TE: 8.4/3.2).

dynamic susceptibility contrast-enhanced-MRI imaging

For DSCE-MR acquisition, all the patients were kept fasting for 3–4 h, and two MR imaging datasets were acquired before and after intravenous administration of Gadopentetate dimeglumine contrast (0.15 mmol/kg). The contrast was injected at a flow rate of 3.0–5.0 mL/min in the antecubital vein by using a power injector through an intravenous catheter followed by a saline flush of 25.0 mL at the same rate. Abnormal contrast enhancement in the tumor-affected site was evaluated in three planes on all the sequences. Postprocessing of DSCE-MRI data was performed utilizing comprehensive neuroimaging software (nordicBrainEx, Nordic Neuro Lab, Norway) including co-registration of DSCE images with anatomical MRI images, leakage correction, vessel removal and normalization.

Parametric maps were generated for precisely calculating the normalized cerebral blood volume (nCBV) values in the tumor areas. The output nCBV maps were normalized for balancing the mean nCBV value of the normal brain tissue as 1.0, whereas the tumor tissue typically had a higher value. nCBV values were calculated in ROIs placed at the tumor areas showing maximum perfusion. To optimize reproducibility, three nCBV measurements were obtained using three different slices of nCBV maps, which were then averaged as the final value for nCBV in the individual patient.

Magnetic resonance spectroscopy imaging

Patients were subjected to multivoxel point resolved two-dimensional chemical shift imaging (2D-CSI) with spectroscopy sequence on tumoral/peritumoral regions to evaluate the pattern for N-acetyl aspartate (NAA), choline (Cho), creatine (Cr) and lipid-lactate metabolites. Water suppression was achieved with a chemically selective suppression pulse sequence. Automated global shimming was used to minimize the B_0 inhomogeneity and localized shimming was done to further minimize B_0 field variations over the voxel of interest. The FLAIR or contrast-enhanced transverse T1-weighted images were used to localize and to place the volume of interest. Siemens and GE healthcare inbuilt software packages were used for processing the MRS data. MRS raw data were transferred to the workstation (Syngo MR Workstation, Siemens, Erlangen, Germany containing B 17 version of the software or GE Healthcare workstation) for postprocessing. The relative metabolite concentration ratios of Cho/NAA, Cho/Cr, Cr/NAA, and Cr/Cho on the tumors were estimated.

Single-photon emission tomography/MRI fusion

The corresponding SPECT and MRIs' fusion was done by using fusion software (Multimodality Oasis Server version 1.9.4.3, Segami Corp., Columbia, Maryland, USA) for the better delineation of the tumor boundaries,

Histopathology and immunohistochemistry

The tissue diagnosis of glioma was established by performing routine histopathological analysis on the biopsied tumor samples. Histopathological grading was done according to the WHO classification system-2007 [15]. The Ki-67 labeling index was evaluated by the standard IHC technique. The percent Ki-67 labeling index was defined as the percentage of nuclei stained positively per the total number of nuclei for Ki-67 nuclear antigens.

Statistical analysis

The statistical analysis was carried out using the Statistical Package for Social Sciences (IBM SPSS statistics 21). The Receiver-operating characteristic (ROC) analysis was performed to obtain the sensitivity and specificity for the quantitative variables reaching statistical significance to differentiate low-grade and high-grade gliomas. The Pearson correlation test was run to test the relationship between MDM SPECT and different MR parameters. All statistical tests were two-sided and were performed at a significance level of $P \leq 0.05$.

Results

Histopathology and immunohistochemistry

Histological examination performed in 29 patients revealed that 13 patients had glioblastoma multiforme (GBM) (G-IV), two patients each had anaplastic astrocytoma and oligodendroglioma (ODG) (G-III), and three patients each had astrocytoma and diffuse astrocytoma (G-II). One patient each had oligoastrocytoma, ODG and gemistocytic astrocytoma (G-II), respectively. Incidentally, three patients with clinical as well as radiological suspicion of glioma during the presurgical evaluation turned out to be meningioma (meningioma – two patients and angiomatous meningioma – one patient) on histopathological analysis. Patients' demographic details and quantitative imaging parameters have been demonstrated in Table 1.

IHC (Ki-67) was performed in 20 out of 29 patients. Among these 20 patients, nine patients were grade-IV, three patients were of grade-III glioma and five patients were of grade-II glioma, respectively. The remaining three patients had meningioma. The Ki-67 labeling index (LI) increased with the grading of glioma and was estimated to be 3.40 ± 3.71 (1–10%), 18.0 ± 8.18 (9–25%) and

Table 1 Patients' demographic details, glioma grading and quantitative imaging parameters

SN	Age/sex	Tumor type/grade	Tumor location	Ki-67 (%)	T/NT	CBV	Cho/NAA	Cho/Cr	Cr/Cho	Cr/NAA
1	52/F	GBM IV	Corpus callosum	25	6.4	12.99	6.37	4.07	0.45	1.54
2	44/M	GBM IV	Occipital (L)	–	4.4	–	–	–	–	–
3	28/M	GBM IV	Parietal (L)	5	6.125	–	–	–	–	–
4	30/M	GBM IV	Frontal (R)	25	5.3					
5	52/F	GBM IV	Corpus callosum	25	4.2	5.337	3.50	2.16	0.45	1.27
6	44/M	GBM IV	Temporal (L)	40	6.76					
7	44/M	GBM IV	Frontal (L)	–	6.5					
8	24/F	GBM IV	Insular glioma (R)	–	4.7	6.43	5.30	3.09	0.32	2.59
9	46/M	GBM IV	Corpus callosum	–	5.57	3.57	1.14	2.30	0.42	2.50
10	50/M	GBM IV	Frontal (L) and (R)	20	3.37	3.30	4.98	1.17	0.84	3.17
11	65/M	GBM IV	Parietal (R)	9	3.48	–	–	–	–	–
12	54/M	GBM IV	Frontal (R)	60	3.9	–	–	–	–	–
13	45/M	GBM IV	Fronto-parietal (R)	9	6.4	–	–	–	–	–
14	30/F	Anaplastic astrocytoma III	Corpus callosum	9	4	–	–	–	–	–
15	37/M	ODG III	Parietal (R)	25	8.6	8.73	6.40	3.60	0.29	1.78
16	57/M	ODG III	Prietotemporal (R)	20	8.714	8.9	9.76	10.50	0.90	3.17
17	47/M	Anaplastic astrocytoma III	Temporal (L) with thalamic extension	–	7.2	–	–	–	–	–
18	45/M	Astrocytoma II	Frontal (R)	–	1.06	1.456	2.40	1.44	0.17	1.56
19	45/M	Oligoastrocytoma II	Insular glioma (R)	2	1.16	1.39	2.31	3.27	0.35	1.72
20	46/M	Diffuse astrocytoma II	Temporal (L)	–	2.8	–	–	–	–	–
21	30/M	Astrocytoma II	Temporal (R)	–	1.1	1.56	3.80	1.57	0.63	1.66
22	40/M	Diffuse astrocytoma II	Frontal (L)	1	0.8	–	–	–	–	–
23	24/M	Astrocytoma II	Insular glioma RT	2	1.8	1.41	3.18	1.24	0.80	2.74
24	47/M	Diffuse astrocytoma II	Multicentre glioma		3.44	3.7	2.50	3.50	0.89	2.89
25	36/F	ODG II	Thalamic gliioma (L)	2	1.9	–	–	–	–	–
26	43/M	Astrocytoma gemistocytic II	Frontoparietal (L)	10	8.1	–	–	–	–	–
27	37/M	Meningioma I	Prietotemporal (L)	1	11.9	–	–	–	–	–
28	32/M	Meningioma I	Parietal (R)	2	12	–	–	–	–	–
29	58/M	Meningioma (angiomatous) I	Frontal (L)	2	23.8	–	–	–	–	–

CBV, cerebral blood volume; Cho, choline; Cr, creatine; F, female; GBM, glioblastoma multiforme; L, left; NAA, N-acetyl aspartate; ODG, oligodendroglioma; R, right; T/NT ratio, target-to-nontarget ratio.

24.22 ± 17.3 (5–60%) in G-II, G-III and G-IV, respectively. The mean ± SD values of Ki-67 in grade-II gliomas were significantly lower as compared to grade III ($P = 0.008$) and grade IV ($P = 0.02$) gliomas. No statistical difference was observed in mean values of Ki-67 LI between glioma grade III and grade IV. In G-IV group of patients, one patient had a Ki-67 value as low as 5.0% which was observed typically seen in G-II glioma. Similarly, the Ki-67 index was also higher (10%) in one patient of gemistocytic astrocytoma (grade II) compared to other grade II glioma. In meningioma, the mean Ki-67 index was estimated to be 1.66 ± 0.57 and ranged between 1.0 and 2.0%.

99mTc-methionine single-photon emission tomography image findings

The radiolabeled product remained stable for up to 24 h. The radiolabeling efficiency for the final product of 99mTc-MDM was evaluated for each kit and the mean value was estimated to be 97.0 ± 1.5%. No adverse effects were observed in any of the patients after intravenous tracer administration.

On 99mTc-MDM SPECT, a focally increased uptake of the radiotracer was seen in 17 HGG (G-III/G-V) patients and was interpreted as disease positive. On the other hand, in LGG (G-II, $n = 9$), positive scan findings were observed in 4/9 patients. In the remaining 5/9 patients, no noticeable tracer uptake was seen, and hence, the findings were interpreted as negative for the detection of any disease activity. However, the findings were false negative in view of the histopathological evidence of LGG (three astrocytoma, one diffuse astrocytoma and one oligoastrocytoma) in this subset of patients. Interestingly, very high tracer uptake (T/NT ratio = 15.9 ± 6.8) was observed in meningiomas. No visible tracer uptake was seen in three control cases. The overall sensitivity, specificity, false positive rate and false negative rate of 99mTc-MDM SPECT to pick the brain neoplasm were estimated to be 86.2, 100, 0.0 and 13.8%, respectively.

Quantitative analysis of 99mTc-methionine single-photon emission tomography and MRI imaging

The mean ± SD values of the T/NT ratio of 99mTc-MDM uptake in glioma grade II, grade III and grade IV patients were estimated to be 2.46 ± 2.3, 7.13 ± 2.2 and 5.16 ± 1.2, respectively. Table 2 presents the T/NT ratios and the corresponding Ki-67 values in different grades of tumors. The mean ± SD values of the T/NT ratio of 99mTc-MDM uptake in meningioma were much higher than that any of glioma variants and were estimated to be 15.9 ± 6.8. Interestingly, the ratio in grade-III tumors was higher than in grade-IV, whereas, in G-II tumors, the ratio was lowest at 2.46 ± 2.3 ($n = 9$). The ratio in low grade (G-II) was estimated to be slightly lower (1.75 ± 0.9), when one patient of gemistocytic astrocytoma (with the T/NT ratio of 8.1) was excluded as an outlier ($n = 8$). A box-and-whisker diagram depicting a significant difference in T/NT ratios in patients with different WHO grades of glioma and meningioma is presented in Fig. 1.

Table 2 The target-to-nontarget ratios (mean ± SD values) and Ki-67 indices in different grades of glioma and meningioma in a subset of 29 patients recruited preoperatively

Histological type/grade	Mean age (years)	99mTc-MDM SPECT T/NT ratio	Ki-67 index
G-IV	44.4 ± 11.3	5.16 ± 1.2 (*n*=13)	24.22 ± 17.3 (*n*=9)
G-III	42.7 ± 11.7	7.13 ± 2.2* (*n*=4)	18.0 ± 8.18 (*n*=3)
G-II	39.12 ± 8.5	1.75 ± 0.9** (*n*=9)	3.40 ± 3.71 (*n*=5)
G-I (meningioma)	46.0 ± 10.8	15.9 ± 6.8** (*n*=3)	1.66 ± 0.57 (*n*=3)

99mTc-MDM, 99mTc-methionine; SPECT, single-photon emission tomography; T/NT ratio, target-to-nontarget ratio.
*P=0.05; **P=0.001.

Fig. 1

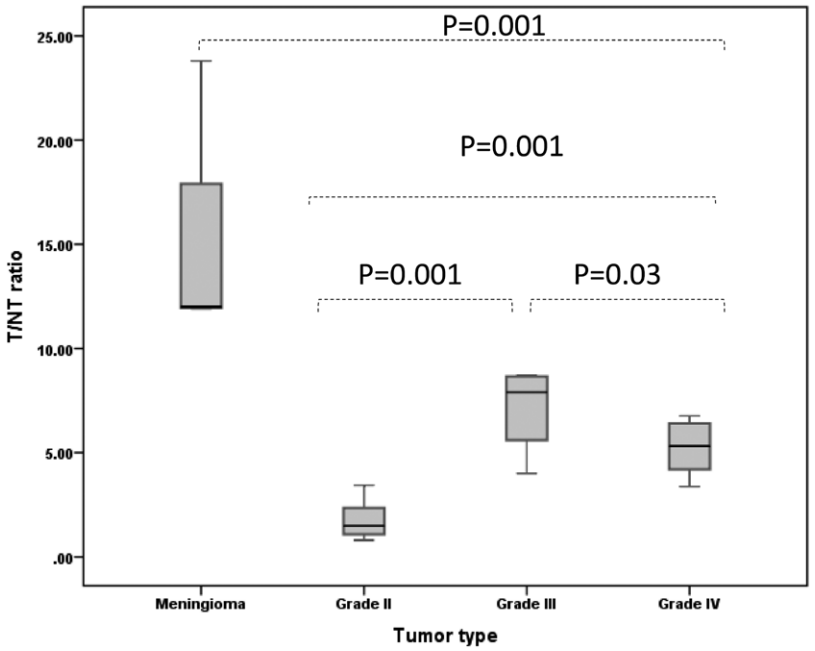

A box-and-whisker diagram depicting a significant difference in T/NT ratios in patients with different grades of glioma and meningioma. T/NT ratio, target-to-nontarget ratio.

Similarly, we observed that the normalized cerebral blood volume (nCBV) as estimated (7.03 ± 3.44) by DSCE-MRI in HGG was significantly (P = 0.001) higher than that (1.90 ± 1.0) observed in LGG patients. Likewise, the Cho/NAA ratio was also significantly (P = 0.04) higher (5.35 ± 2.67) in HGG than (2.83 ± 0.63) in LGG patients. The remaining MRS quantification parameters, that is, Cho/Cr, Cr/NAA and Cr/Cho did not differ significantly among the two groups (HGG versus LGG) of patients (Table 3). Representatives of SPECT, DSCE-MR, MRS images used for evaluation of quantitative functional parameters in a freshly diagnosed HGG patient are presented in Fig. 2. A case example of 99mTc-MDM SPECT in a rare case of gemistocytic astrocytoma exhibiting high T/NT ratio of 8.1 is presented in Fig. 3.

The ROC analysis (Fig. 4) estimated a T/NT cutoff value of 3.08 which provided 100% sensitivity and 87.5% specificity in discriminating between HGG and LGG. Likewise, an nCBV cutoff ratio of 2.42 achieved 100.0% sensitivity and 80.0% specificity. Similarly, the cutoff ratio of 3.34 of Cho/NAA offered sensitivity and specificity of 85.7 and 80.0%, respectively, for this discrimination.

Association of target-to-nontarget ratios with magnetic resonance quantification parameters and Ki-67 index:
The Pearson correlation (two-tailed) analysis demonstrated a positive correlation between the T/NT ratio and nCBV (r = 0.90; P < 0.0001), Cho/NAA (r = 0.762; P = 0.002) and Cho/Cr (r = 0.653; P = 0.01). No significant correlation was observed between T/NT versus Cr/Cho and T/NT versus Cr/NAA, respectively. Similarly, there was no significant correlation between the T/NT ratio and Ki-67 LI (r = 0.33, P = 0.247).

Discussion

In the current study, we analyzed differences in 99mTc-MDM uptake ratios among HGG and LGG lesions in newly diagnosed gliomas and compared with

Table 3 Quantitative 99mTc-methionine single-photon emission tomography and dynamic susceptibility contrast-enhanced-MRI and magnetic resonance spectroscopy data (mean ± SD) in HGG and LGG patients

Quantitative parameter (mean ± SD)	HGG (n=7)	LGG (n=5)	P value
T/NT ratio	5.93 ± 2.09	1.71 ± 1.01	0.007*
CBV ratio	7.03 ± 3.44	1.90 ± 1.0	0.001*
Cho/NAA	5.35 ± 2.67	2.83 ± 0.63	0.04*
Cho/Cr	3.84 ± 3.09	2.20 ± 1.08	0.23
Cr/NAA	2.28 ± 0.76	2.11 ± 0.64	0.35
Cr/Cho	0.41 ± 0.23	0.57 ± 0.30	0.67

CBV, cerebral blood volume; Cho, choline; Cr, creatine; NAA, N-acetyl aspartate; T/NT ratio, target-to-nontarget ratio.
*$P \leq 0.05$.

DSCE-MRI/MRS parameters and Ki-67 proliferation index. The current study was the first-ever clinical study using 99mTc-MDM SPECT ratios comparing and correlating with the cell proliferation index and quantitative MRI. The results of this study have been presented previously as a conference abstract highlighting that 99mTc-MDM uptake differs significantly among LGG and HGG [16]. 99mTc-MDM findings were positive in all the 17 HGG patients, whereas, in LGG, the findings were positive in 4 (4/9) and negative in 5 (5/9) patients, respectively. The tracer therefore offered better diagnostic sensitivity for the detection of HGG than LGG. The false-negative findings in astrocytoma grade-II corroborated with the previously reported studies using 11C-methionine and 18F-fluoro-ethyl-tyrosine (FET) PET which have demonstrated similar findings that a proportion of LGG provides a poor image contrast [17–20]. It has been suggested that an accurate imaging of nonenhancing LGG remains a challenge as these tumors lack neoangiogenesis and cellularity is relatively low in these tumors [21]. In an extensive study, Kracht *et al.* [19] reported that 11C-MET/PET had false-negative findings in 23.0% of low-grade astrocytoma, and thereby presented a limited diagnostic accuracy of this technique in this subset of patients. Interestingly, no false-positive findings were observed on 99mTc-MDM SPECT in patients with cerebral tuberculoma and neurocysticercosis [19]. This finding supports the specificity of 99mTc-MDM for brain tumors. However, a mild methionine uptake of 11C-MET has been observed in a small number of inflammatory lesions and acute demyelination [19,21,22]. Similarly, such a nonspecific uptake of 18F-FET in non-neoplastic brain lesions have also been reported [23,24]. It has been suggested that cancer cells may have a higher abnormal requirement for methionine for their aberrant excess trans-methylation [25]. Haining *et al.* [26] showed that LAT1 receptors are overexpressed in human gliomas, thereby suggesting that LAT1 expression is closely associated with the formation and development of gliomas and thus LAT1 receptors could be considered as one of the potential molecular targets in glioma detection as well as therapy [12,13].

The quantitative results of our study to differentiate HGG from LGG were found to agree with the findings of previous 11C-MET PET studies which demonstrated a significant difference in the 11C-methionine uptake values between high-grade and low-grade tumors [11,27]. Our study findings showed that 99mTc-MDM tracer uptake increases with increasing glioma grading when excluding anaplastic ODGs and the differences in MDM uptake are more evident between glioma grade-II and grade-IV and grade-II and grade-III than between glioma grade-III and grade-IV. Similar to our results, Singhal *et al.* [11] reported a significant difference in the maximum 11C-MET PET standardized uptake value between glioma grade-II and grade-IV (P=0.005) and between grade-III and grade-IV (P=0.03) [11].

The higher mean T/NT ratio of 99mTc-MDM in grade-III glioma in the present study was probably due to the ODG component as it has been reported earlier that ODGs exhibit a higher methionine uptake [28,29]. It has been reported previously that 11C-MET uptake and tumor vascularization are inter-related. The microvessel density in grade-II ODG is higher than that in GBM [29]. Furthermore, Kracht *et al.* [28] reported that 11C-MET PET in glioma serves as a direct measure of methionine amino acid transport and acts as a surrogate marker of microvessel density within the gliomas. Therefore, angiogenesis and 11C-MET uptake seem to be closely associated events in gliomas [29]. Subsequently, Manabe *et al.* [30] investigated metabolic 11C-MET PET and correlation with pathological grading with and without the oligodendroglial component and observed that this separation improved the detection accuracy between LGG and HGG.

Likewise, nCBV, Cho/NAA and Cho/Cr ratios were also observed to be higher in grade III ODGs than in any other glioma variant. Saito *et al.* [31] showed that the mean relative CBV (rCBV) in astrocytic tumors excluding GBM was significantly lower than that observed in oligodendroglial tumors. This finding is not perfectly in agreement with our findings as T/NT, and nCBV ratios were higher in ODG grade III than any other glioma variant [31]. Similarly, the patients with ODG had been reported to have a high intensity of Cho signals [32,33]. A higher Cho level in ODGs is attributed to the histopathological evidence that oligodendrocytes are involved in myelin membrane synthesis and repair process, which utilizes choline metabolite for this synthesis [34]. The observation of the highest uptake in our study in meningioma cases (n=3) could be due to the increased LAT-1 expression as meningiomas are reported to have high angiogenesis, increased vascularity and LAT-1 overexpression [18,28]. In support of these findings, 11C-methionine has also been reported to have high but variable uptake in meningioma [35]. This variability in methionine amino acid uptake is in line with our results

Fig. 2

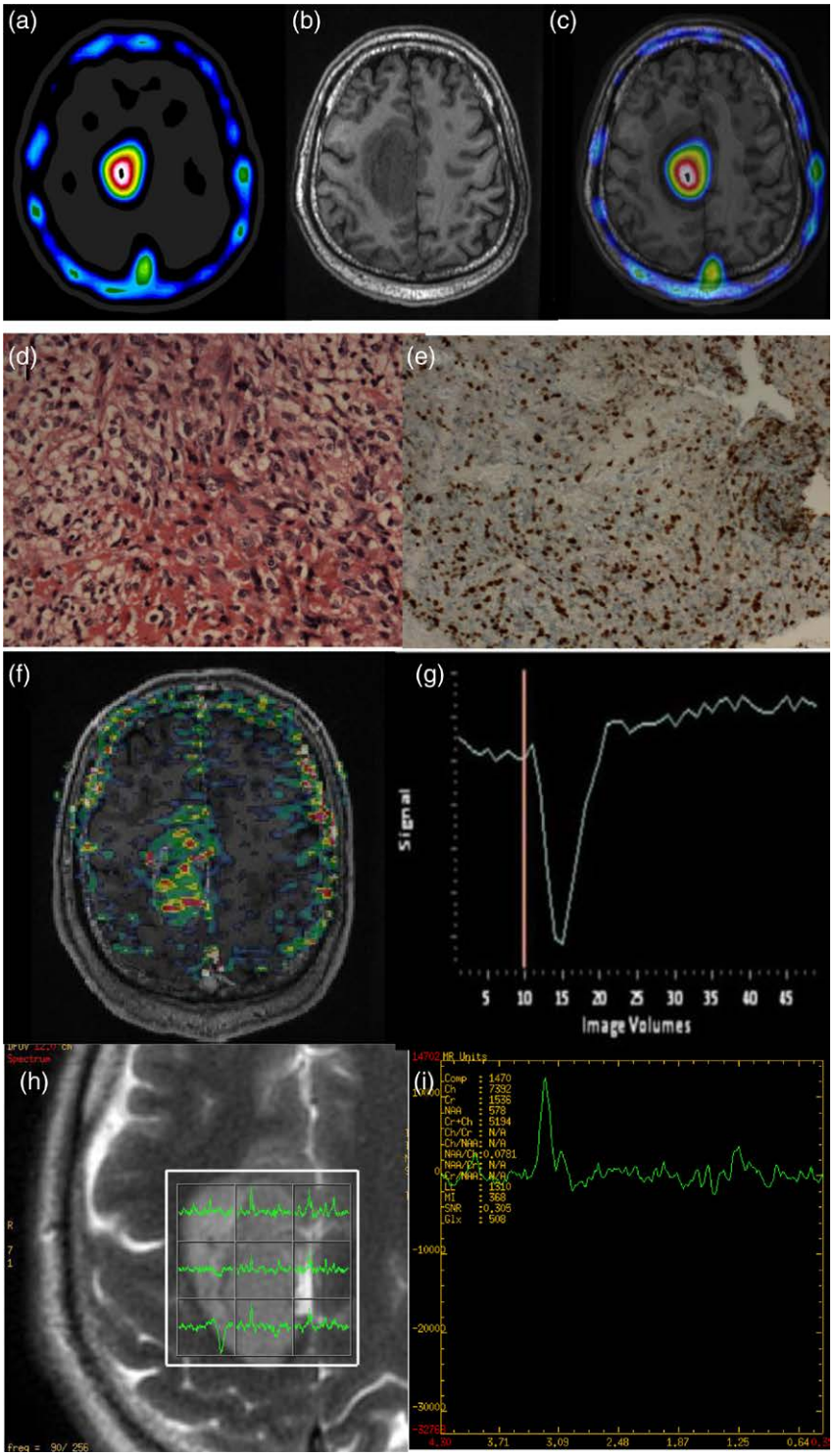

99mTc-MDM SPECT (a) image preoperatively in a 57-year-old male patient with anaplastic ODG (G-III) having symptoms of headache and hemiparesis demonstrating intense tracer uptake (T/NT ratio=8.71) in the right parietotemporal region. Concordant MR lesion enhancement and signal change (b]) in T1-FLAIR axial image and (c) SPECT/MR fused transaxial slice. Histopathological findings (d and e) showing densely cellular tumor with prominent nuclear pleomorphism, mitotic activity and increased vascularity and high proliferation index (Ki-67 LI=20.0%). DSCE-MRI imaging derived cerebral CBV-map (f) showing high perfusion (nCBV ratio=8.9). The characteristic T2 signal intensity perfusion curve (g) and multivoxel MRS (h) showing a high Cho peak and a reduced NAA peak (i). 99mTc-MDM, 99mTc-methionine; CBV, cerebral blood volume; Cho, choline; DSCE, dynamic susceptibility contrast enhanced; GBM, glioblastoma multiforme; MRS, magnetic resonance spectroscopy; NAA, N-acetyl aspartate; ODG, oligodendroglioma; SPECT, single-photon emission tomography; T/NT ratio, target-to-nontarget ratio.

Fig. 3

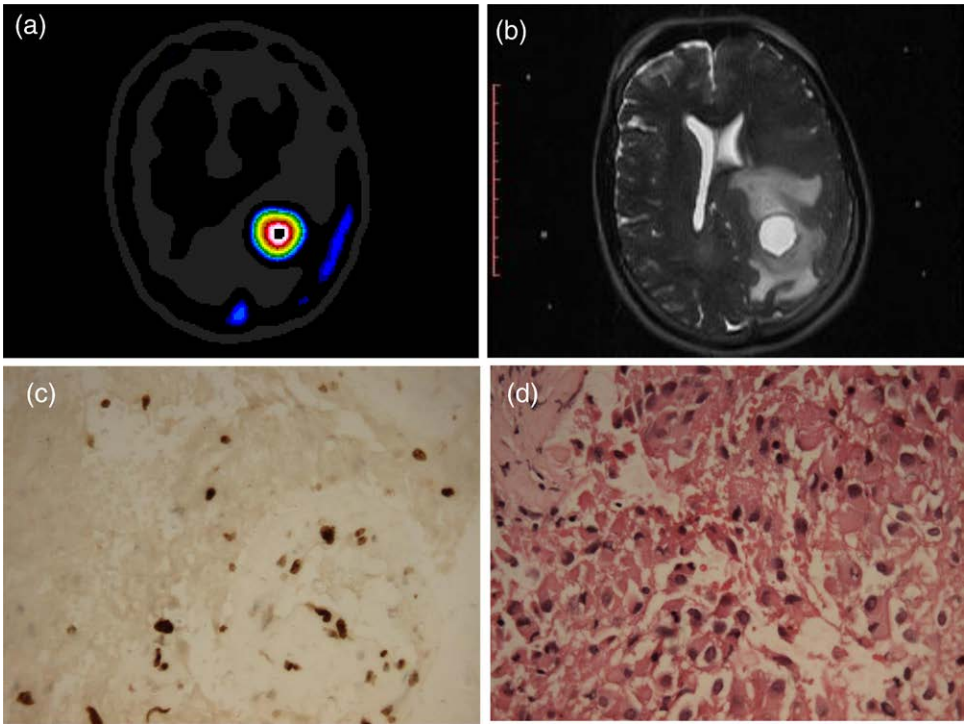

99mTc-MDM SPECT (a) showing intense and focal tracer uptake (T/NT ratio=8.1) in the left parietal region in a 43–year-old male patient with gemistocytic astrocytoma (Grade-II). Contrast MRI T2-weighted MR (b) showing lesion enhancement in the corresponding region. Histopathological analysis (H&E, 400×) results (c) showing inconspicuous nuclei and abundant eosinophilic cytoplasmic giving gemistocytic appearance with no mitosis, necrosis or endothelial proliferation. IHC (d) showing moderate proliferation index (Ki-67 LI) of 10.0%. 99mTc-MDM, 99mTc-methionine; SPECT, single-photon emission tomography; T/NT ratio, target-to-nontarget ratio.

Fig. 4

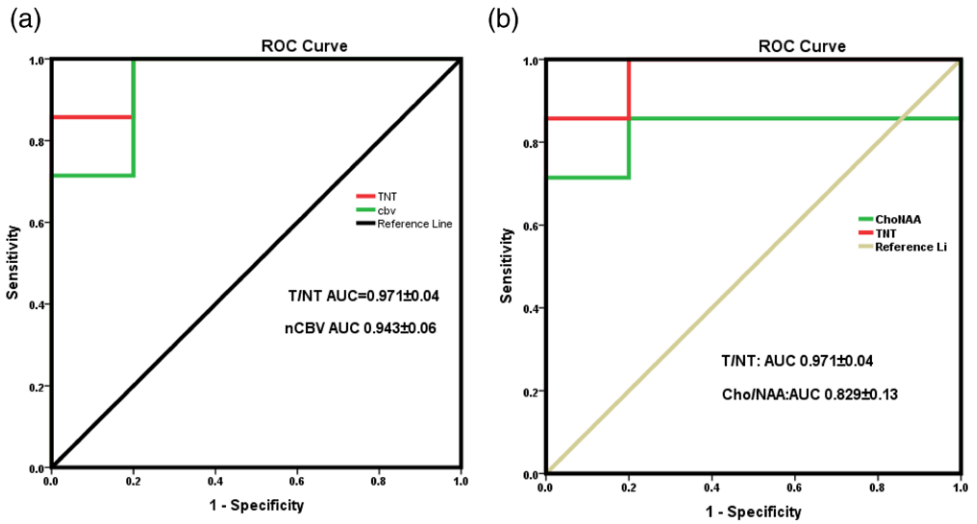

The ROC curve analysis comparing sensitivity and specificity of the T/NT ratio with nCBV (a) and Cho/NAA (b) for the accurate differentiation of high-grade from low-grade glioma. Cho, choline; nCBV, normalized cerebral blood volume; NAA, N-acetyl aspartate; ROC, receiver-operating characteristic; T/NT ratio, target-to-nontarget ratio.

because the 99mTc-MDM uptake ratio range was varied from 11.90 to 23.80. Furthermore, we observed homogenous 99mTc-MDM uptake in two cases of meningioma, whereas a heterogeneous distribution in one case of angiomatous meningioma subtype. Previously, Nyberg *et al.* [35] described a homogenous 11C-MET uptake in meningiomas, whereas Luchi *et al.* [36] reported a heterogeneous distribution of amino acid uptake. It is therefore evident that 99mTc-MDM may be an extremely useful tracer for distinguishing noninvasively meningioma from glioma and other CNS tumors at the initial diagnostic work-up prior to the surgery.

The histopathological analysis (Fig. 3) showed inconspicuous nuclei and abundant eosinophilic cytoplasmic giving gemistocytic appearance with no mitosis, necrosis or endothelial proliferation, but demonstrated high tracer uptake and image contrast. This tumor type is graded as WHO-grade-II; however, on IHC, it turned out to be 'like high grade' with a Ki-67 labeling index of 10.0%. The relevance of recognition of this variant is related to its association with aggressive biological behavior due to its increased tendency for rapid progression to GBM and recurrence [37]. It has been previously reported that gemistocytic can progress toward anaplastic astrocytoma and glioblastoma earlier than other low-grade gliomas. Thus, it has been suggested that all gemistocytic astrocytomas be clinically managed as grade III anaplastic astrocytoma, and probably may even be reclassified [38]. Our finding is in concordance with these studies. Furthermore, methionine uptake in glioma has been suggested to be correlated with the cell proliferation and Ki-67 expression [27,28,39]. We found a significant difference in the mean T/NT ratios and Ki-67 values in different grades of glioma. However, no overall significant correlation was found between T/NT ratios and Ki-67 values. The published results have reported confounding results, some indicating a correlation between methionine and Ki-67 values and others demonstrating no such correlation [28,39,40].

Furthermore, we observed that the area of hyperperfusion as seen on DSCE-MR matched identically with the high methionine uptake regions on 99mTc-MDM SPECT. Consequently, we found a very strong correlation ($r = 0.90$; $P < 0.0001$) between nCBV values and T/NT ratios. This observation is in complete agreement with a previous report by Sadeghi *et al.* [41] who found a strong correlation ($r = 0.89$, $P = 0.00001$) between rCBV values and 11C MET uptake values in a group of 18 glioma patients [42].

We observed increased nCBV and methionine uptake in ODG and meningiomas, but these patients responded to treatment and have shown better survival than malignant astrocytomas. Similar observations have been made in previous studies that high perfusion and methionine uptake are not always indicative of the highly aggressive tumor behavior [42,43]. Likewise, we found a significant correlation between the T/NT ratio and Cho/NAA ($r = 0.762$; $P = 0.002$) and Cho/Cr ($r = 0.653$; $P = 0.01$) ratios. Correlative imaging using MRS and amino acid-based PET/SPECT has been scarcely used in glioma. These limited studies have recently used 2D/3D multivoxel spectroscopy in combination with 18F-FET PET imaging and found a correlation between FET uptake and Cho/NAA which was in agreement with our study [44,45].

Conclusion

Quantitative preoperative 99mTc-MDM SPECT provided high sensitivity and specificity to differentiate HGG versus LGG and demonstrated a potential role for the differential diagnosis of glial versus nonglial tumors. 99mTc-MDM SPECT can be incorporated (in combination with conventional MRI) as an accurate technique in the presurgical diagnostic work-up in glioma patients at an affordable cost for glioma characterization. The study, however, needs to be done in a large cohort of patients.

Acknowledgements:

B.S. acknowledges the financial grant by the Institute of Nuclear Medicine & Allied (INMAS), DRDO, MOD, Delhi, India as an extramural project to him to conduct this study at PGIMER, Chandigarh, India. N.R. acknowledges the grant of research fellowship by the Indian Council of Medical Research (ICMR), Ministry of Health, Government of India.

Conflicts of interest

There are no conflicts of interest.

References

1 Wrensch M, Minn Y, Chew T, Bondy M, Berger MS. Epidemiology of primary brain tumors: current concepts and review of the literature. *Neuro Oncol* 2002; **4**:278–299.
2 Glantz MJ, Burger PC, Herndon JE II, Friedman AH, Cairncross JG, Vick NA, Schold SC Jr. Influence of the type of surgery on the histologic diagnosis in patients with anaplastic gliomas. *Neurology* 1991; **41**:1741–1744.
3 Verburg N, Hoefnagels FWA, Barkhof F, Boellaard R, Goldman S, Guo J, *et al.* Diagnostic accuracy of neuroimaging to delineate diffuse gliomas within the brain: a meta-analysis. *AJNR Am J Neuroradiol* 2017; **38**:1884–1891.
4 Filss CP, Cicone F, Shah NJ, Galldiks N, Langen KJ. Amino acid PET and MR perfusion imaging in brain tumours. *Clin Transl Imaging* 2017; **5**:209–223.
5 Law M, Yang S, Wang H, Babb JS, Johnson G, Cha S, *et al.* Glioma grading: sensitivity, specificity, and predictive values of perfusion MR imaging and proton MR spectroscopic imaging compared with conventional MR imaging. *AJNR Am J Neuroradiol* 2003; **24**:1989–1998.
6 Lev MH, Ozsunar Y, Henson JW, Rasheed AA, Barest GD, Harsh GR, *et al.* Glial tumor grading and outcome prediction using dynamic spin-echo MR susceptibility mapping compared with conventional contrast-enhanced MR: confounding effect of elevated rCBV of oligodendroglimoas. *AJNR Am J Neuroradiol* 2004; **25**:214–221.
7 Belliveau JG, Bauman G, Macdonald DR. Detecting tumor progression in glioma: current standards and new techniques. *Expert Rev Anticancer Ther* 2016; **16**:1177–1188.
8 Singhal T, Narayanan TK, Jain V, Mukherjee J, Mantil J. 11C-L-methionine positron emission tomography in the clinical management of cerebral gliomas. *Mol Imaging Biol* 2008; **10**:1–18.
9 Yanagida O, Kanai Y, Chairoungdua A, Kim DK, Segawa H, Nii T, *et al.* Human L-type amino acid transporter 1 (LAT1): characterization of

function and expression in tumor cell lines. *Biochim Biophys Acta* 2001; **1514**:291–302.
10 Kim DK, Kim IJ, Hwang S, Kook JH, Lee MC, Shin BA, *et al*. System L-amino acid transporters are differently expressed in rat astrocyte and C6 glioma cells. *Neurosci Res* 2004; **50**:437–446.
11 Singhal T, Narayanan TK, Jacobs MP, Bal C, Mantil JC. 11C-methionine PET for grading and prognostication in gliomas: a comparison study with 18F-FDG PET and contrast enhancement on MRI. *J Nucl Med* 2012; **53**:1709–1715.
12 Singh B, Kumar N, Sharma S, Watts A, Hazari PP, Rani N, *et al*. 99mTc-MDM brain SPECT for the detection of recurrent/remnant glioma-comparison with ceMRI and 18F-FLT PET imaging: initial results. *Clin Nucl Med* 2015; **40**:e475–e479.
13 Hazari PP, Shukla G, Goel V, Chuttani K, Kumar N, Sharma R, Mishra AK. Synthesis of specific SPECT-radiopharmaceutical for tumor imaging based on methionine: 99mTc-DTPA-bis(methionine). *Bioconjug Chem* 2010; **21**:229–239.
14 Rani N, Singh B, Kumar N, Singh P, Hazari PP, Singh H, *et al*. Differentiation of recurrent/residual glioma from radiation necrosis using semi quantitative 99mTc MDM (bis-methionine-DTPA) brain SPECT/CT and dynamic susceptibility contrast-enhanced MR perfusion: a comparative study. *Clin Nucl Med* 2018; **43**:e74–e81.
15 Louis DN, Ohgaki H, Wiestler OD, Cavenee WK, Burger PC, Jouvet A, *et al*. The 2007 WHO classification of tumours of the central nervous system. *Acta Neuropathol* 2007; **114**:97–109.
16 Rani N, Singh B, Hazari PP, Singh P, Kumar N, Kumar SG, *et al*. [99MTC]-MDM SPECT as a prognostic marker for pre-operative and post-operative serial evaluation of glioma compared with DSCE-MRI and 1H-MRS. *J Neurol Sci* 2019; **405**:108–109.
17 Gumprecht H, Grosu AL, Souvatsoglou M, Dzewas B, Weber WA, Lumenta CB. 11C-Methionine positron emission tomography for preoperative evaluation of suggestive low-grade gliomas. *Zentralbl Neurochir* 2007; **68**:19–23.
18 Torii K, Tsuyuguchi N, Kawabe J, Sunada I, Hara M, Shiomi S. Correlation of amino-acid uptake using methionine PET and histological classifications in various gliomas. *Ann Nucl Med* 2005; **19**:677–683.
19 Kracht LW, Miletic H, Busch S, Jacobs AH, Voges J, Hoevels M, *et al*. Delineation of brain tumor extent with [11C]L-methionine positron emission tomography: local comparison with stereotactic histopathology. *Clin Cancer Res* 2004; **10**:7163–7170.
20 Rapp M, Heinzel A, Galldiks N, Stoffels G, Felsberg J, Ewelt C, *et al*. Diagnostic performance of 18F-FET PET in newly diagnosed cerebral lesions suggestive of glioma. *J Nucl Med* 2013; **54**:229–235.
21 Floeth FW, Pauleit D, Sabel M, Stoffels G, Reifenberger G, Riemenschneider MJ, *et al*. Prognostic value of O-(2-18F-fluoroethyl)-L-tyrosine PET and MRI in low-grade glioma. *J Nucl Med* 2007; **48**:519–527.
22 Miyake K, Ogawa D, Okada M, Hatakeyama T, Tamiya T. Usefulness of positron emission tomographic studies for gliomas. *Neurol Med Chir (Tokyo)* 2016; **56**:396–408.
23 Jansen NL, Graute V, Armbruster L, Suchorska B, Lutz J, Eigenbrod S, *et al*. MRI-suspected low-grade glioma: is there a need to perform dynamic FET PET? *Eur J Nucl Med Mol Imaging* 2012; **39**:1021–1029.
24 Floeth FW, Pauleit D, Wittsack HJ, Langen KJ, Reifenberger G, Hamacher K, *et al*. Multimodal metabolic imaging of cerebral gliomas: positron emission tomography with [18F]fluoroethyl-L-tyrosine and magnetic resonance spectroscopy. *J Neurosurg* 2005; **102**:318–327.
25 Hoffman RM. l-[Methyl-11 C] methionine-positron-emission tomography (MET-PET). In: Hoffman RM, editor, *Methionine Dependence of Cancer and Aging: Methods and Protocols, Methods in Molecular Biology,* vol. 1866. New York, NY: Humana Press; 2019. https://doi.org/10.1007/978-1-4939-8796-2_20.
26 Haining Z, Kawai N, Miyake K, Okada M, Okubo S, Zhang X, *et al*. Relation of LAT1/4F2hc expression with pathological grade, proliferation and angiogenesis in human gliomas. *BMC Clin Pathol* 2012; **12**:4.
27 Tanaka K, Yamamoto Y, Maeda Y, Yamamoto H, Kudomi N, Kawai N, *et al*. Correlation of 4'-[methyl-(11)C]-thiothymidine uptake with Ki-67 immunohistochemistry and tumor grade in patients with newly diagnosed gliomas in comparison with (11)C-methionine uptake. *Ann Nucl Med* 2016; **30**:89–96.
28 Kracht LW, Friese M, Herholz K, Schroeder R, Bauer B, Jacobs A, *et al*. Methyl-[11 C]-l-methionine uptake as measured by positron emission tomography correlates to microvessel density in patients with glioma. *Eur J Nucl Med Mol Imaging* 2003; **30**:868–873.
29 Chan AS, Leung SY, Wong MP, Yuen ST, Cheung N, Fan YW, Chung LP. Expression of vascular endothelial growth factor and its receptors in the anaplastic progression of astrocytoma, oligodendroglioma, and ependymoma. *Am J Surg Pathol* 1998; **22**:816–826.
30 Manabe O, Hattori N, Yamaguchi S, Hirata K, Kobayashi K, Terasaka S, *et al*. Oligodendroglial component complicates the prediction of tumour grading with metabolic imaging. *Eur J Nucl Med Mol Imaging* 2015; **42**:896–904.
31 Saito T, Yamasaki F, Kajiwara Y, Abe N, Akiyama Y, Kakuda T, *et al*. Role of perfusion-weighted imaging at 3T in the histopathological differentiation between astrocytic and oligodendroglial tumors. *Eur J Radiol* 2012; **81**:1863–1869.
32 McKnight TR. Proton magnetic resonance spectroscopic evaluation of brain tumor metabolism. *Semin Oncol* 2004; **31**:605–617.
33 Gupta RK, Cloughesy TF, Sinha U, Garakian J, Lazareff J, Rubino G, *et al*. Relationships between choline magnetic resonance spectroscopy, apparent diffusion coefficient and quantitative histopathology in human glioma. *J Neurooncol* 2000; **50**:215–226.
34 Nunn AV, Barnard ML, Bhakoo K, Murray J, Chilvers EJ, Bell JD. Characterisation of secondary metabolites associated with neutrophil apoptosis. *FEBS Lett* 1996; **392**:295–298.
35 Nyberg G, Bergström M, Enblad P, Lilja A, Muhr C, Långström B. PET-methionine of skull base neuromas and meningiomas. *Acta Otolaryngol* 1997; **117**:482–489.
36 Iuchi T, Iwadate Y, Namba H, Osato K, Saeki N, Yamaura A, Uchida Y. Glucose and methionine uptake and proliferative activity in meningiomas. *Neurol Res* 1999; **21**:640–644.
37 Avninder S, Sharma MC, Deb P, Mehta VS, Karak AK, Mahapatra AK, Sarkar C. Gemistocytic astrocytomas: histomorphology, proliferative potential and genetic alterations–a study of 32 cases. *J Neurooncol* 2006; **78**:123–127.
38 Heo YJ, Park JE, Kim HS, Lee JY, Nam SJ, Jung SC, *et al*. Prognostic relevance of gemistocytic grade II astrocytoma: gemistocytic component and MR imaging features compared to non-gemistocytic grade II astrocytoma. *Eur Radiol* 2017; **27**:3022–3032.
39 Langen KJ, Mühlensiepen H, Holschbach M, Hautzel H, Jansen P, Coenen HH. Transport mechanisms of 3-[123I]iodo-alpha-methyl-L-tyrosine in a human glioma cell line: comparison with [3H]methyl]-L-methionine. *J Nucl Med* 2000; **41**:1250–1255.
40 Kim S, Chung JK, Im SH, Jeong JM, Lee DS, Kim DG, *et al*. 11 C-methionine PET as a prognostic marker in patients with glioma: comparison with 18 F-FDG PET. *Eur J Nucl Med Mol Imaging* 2005; **32**:52–59.
41 Sadeghi N, Salmon I, Tang BN, Denolin V, Levivier M, Wikler D, *et al*. Correlation between dynamic susceptibility contrast perfusion MRI and methionine metabolism in brain gliomas: preliminary results. *J Magn Reson Imaging* 2006; **24**:989–994.
42 Verger A, Filss CP, Lohmann P, Stoffels G, Sabel M, Wittsack HJ, *et al*. Comparison of 18 F-FET PET and perfusion-weighted MRI for glioma grading: a hybrid PET/MR study. *Eur J Nucl Med Mol Imaging* 2017; **44**:2257–2265.
43 Vaquero J, Zurita M, Coca S, Oya S, Morales C. Prognostic significance of clinical and angiogenesis-related factors in low-grade oligodendrogliomas. *Surg Neurol* 2000; **54**:229–234; discussion 234.
44 Stadlbauer A, Prante O, Nimsky C, Salomonowitz E, Buchfelder M, Kuwert T, *et al*. Metabolic imaging of cerebral gliomas: spatial correlation of changes in O-(2-18F-fluoroethyl)-L-tyrosine PET and proton magnetic resonance spectroscopic imaging. *J Nucl Med* 2008; **49**:721–729.
45 Mauler J, Maudsley AA, Langen KJ, Nikoubashman O, Stoffels G, Sheriff S, *et al*. Spatial relationship of glioma volume derived from 18F-FET PET and volumetric MR spectroscopy imaging: a hybrid PET/MRI study. *J Nucl Med* 2018; **59**:603–609.